Supplementary materials

Enhanced activity and sulfur resistance on Cu- and Fe-modified activated carbon for the reduction of NO by CO from regeneration gas

Zhicheng Xu[a, b], Yuran Li[a] *, Yuting Lin[a], Bin Wang[a], Panting Gao[d], Tingyu Zhu[a, b*]

[a] CAS Key Laboratory of Green Process and Engineering, Institute of Process Engineering, Innovation Academy for Green Manufacture, Chinese Academy of Sciences, Beijing 100190, China

[b] Center for Excellence in Regional Atmospheric Environment, Institute of Urban Environment, Chinese Academy of Sciences, Xiamen 361021, China

[c] University of Chinese Academy of Sciences, Beijing 100049, China

[d] State Key Laboratory of Clean and Efficient Coal Utilization, Taiyuan University of Technology, Taiyuan 030024, China

Keywords: NO reduction, carbon monoxide, activated carbon, transition metal modification, SO_2 resistance.

1. Characterization

1.1 Content of metals

The details of various characterizations are shown as follows. For X-ray fluorescence (XRF), 0.5 g samples and 1.5 g soluble starch were mixed and ground into powder, and then 1 g boric acid was added and ground into a wafer for testing. For inductively coupled plasma atomic emission spectrometry (ICP-AES), 0.2 g samples were added to nitric acid for digestion, and a nitric acid solution with completely dissolved metal ions was detected.

1.2 Pore structure

For pore characteristics, the dried sample was degassed at 300 °C for 10 h and then measured in N_2 at -196 °C with relative pressure (p/p_0) in the range of 10^{-7}–1. The specific surface area (S_{BET}) was calculated by the multipoint Brunauer-Emmett-Teller (BET) equation. The total pore volume (V_T) was determined by the N_2 adsorption capacity at $p/p_0 = 0.95$.

1.3 Valence of metals and type of oxygen species

For X-ray photoelectron spectroscopy (XPS), Al Kα target was used; the analysis depth was approximately 10 nm; the resolution was 0.8 eV, and the power was 150 W. The C 1s main peak position at 284.8 eV was used for binding energy calibration. The areas of the main peaks for O 1s, S 2p, Cu 2p, and Fe 2p were detected with the binding

energy error of each peak was $\pm$ 0.2 eV, and the species content of each group was calculated using the Gaussian-Lorentzian deconvolution method.

1.4 Contact angles

For the test of contact angles, the mixed powder was pressed on a tableting machine to form pieces with a thickness of approximately 5 mm with the pressure of the tablet press set to 30 MPa, and then the pieces were placed under the contact angle meter for measurement. Before the test, the sample was ground to powder and mixed with 30 wt% TiO_2 to improve the adhesion of AC. The contact angle of TiO_2 used for binder is 12.8°. The images were recorded using a digital camera, with deionized water as the contact solution.

1.5 Density functional theory (DFT) calculations

For the density functional theory (DFT) calculations, the equilibrium lattice constant of the hexagonal graphene unit cell separated by a vacuum layer at a depth of 15 Å was optimized when using a 15×15×1 Monkhorst-Pack k-point grid for Brillouin zone sampling to be a=2.468 Å. Then, it was used to construct an edged graphene sheet model with p(4x6) periodicity in the x and y directions and 1 atomic layer in the z direction by vacuum depth of 15 Å to separate the surface slab from its periodic duplicates. The edged C atoms were saturated by H atoms. During structural optimizations, the gamma point in the Brillouin zone was used for k-point sampling, and all atoms were allowed to relax.

1.6 Temperature-programmed desorption (TPD) and temperature-programmed reduction (TPR)

The pretreatment and desorption or reaction conditions of TPD and TPR are shown in Table. S1.

Table S1 The pretreatment and desorption or reaction conditions of TPD and TPR

Test		Pretreatment condition	Desorption or reaction condition
TPD	CO-TPD	A 0.03 g sample was degassed at 300 °C for 1 h, cooled to 50 °C for 1 h, and adsorbed in 10% CO/N$_2$ or N$_2$ atmosphere for 1 h.	Raised from 50 °C to 800 °C with a heating rate of 10 °C/min in N$_2$
	NO-TPD	A 0.5 g sample was adsorbed in 500pm NO/N$_2$ and stabilized in N$_2$ at 50 °C for 30 min.	
	SO$_2$-TPD	A 0.5 g sample after NO-CO reaction with SO$_2$ was pretreated under N$_2$ at 50 °C for 30 min.	
TPR	H$_2$-TPR	A 0.05 g sample was pretreated at 300 °C in Ar for 1 h and cooled to 50 °C for 30 min.	Raised from 50 °C to 900 °C with a heating rate of 10 °C/min in N$_2$

1.7 In situ diffuse reflectance infrared Fourier transform spectroscopy (in situ DRIFTS)

For each test, a 0.01 g sample was mixed with 0.20 g KBr and ground into powder. For the reaction spectrum, the sample was first pretreated at 250 °C under a N_2 atmosphere for 1 h, and then the background was collected. Then, the sample underwent first adsorption in a 500 ppm NO atmosphere, then reacted in a 500 ppm CO atmosphere, and last in 500 ppm NO and 500 ppm CO atmospheres. Each step lasted 15 min and collected spectra. For the adsorption spectrum, the sample was first pretreated at 450 °C under a N_2 atmosphere for 1 h, and the background was collected at 450 °C, 350 °C, and 250 °C in turn. Then, the NO adsorption spectra at 250 °C, 350 °C, and 450 °C under 500 ppm NO were successively measured for 15 min with the corresponding background. The flow rate of each step was 100 mL/min.

2. Results and discussion
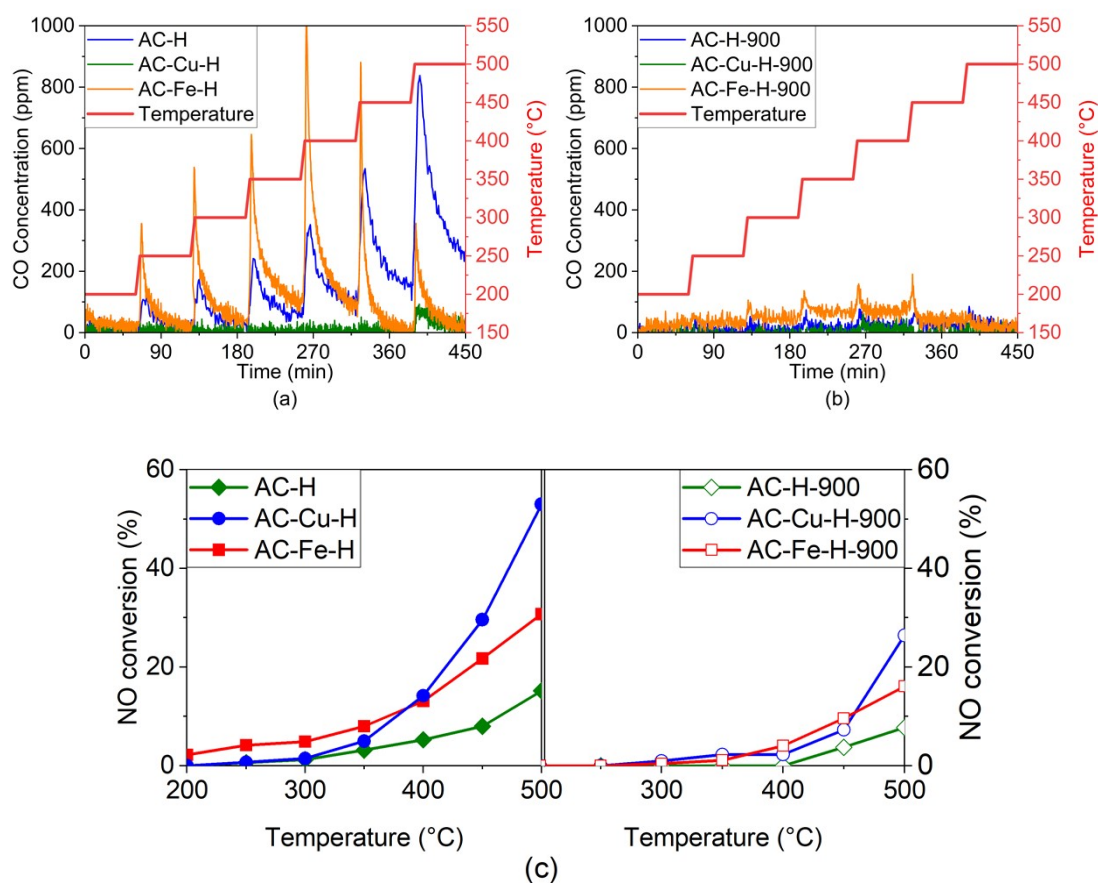
Figure S1 The CO concentration in outlet gas on AC-H and AC-Me-H with (a) or without (b) calculation at 900 °C, and (c) NO conversion of AC-H and AC-Me-H with and without calculation at 900 °C without CO. (Conditions: 500 ppm NO and N_2, 6000 h^{-1}, 200–500 °C).
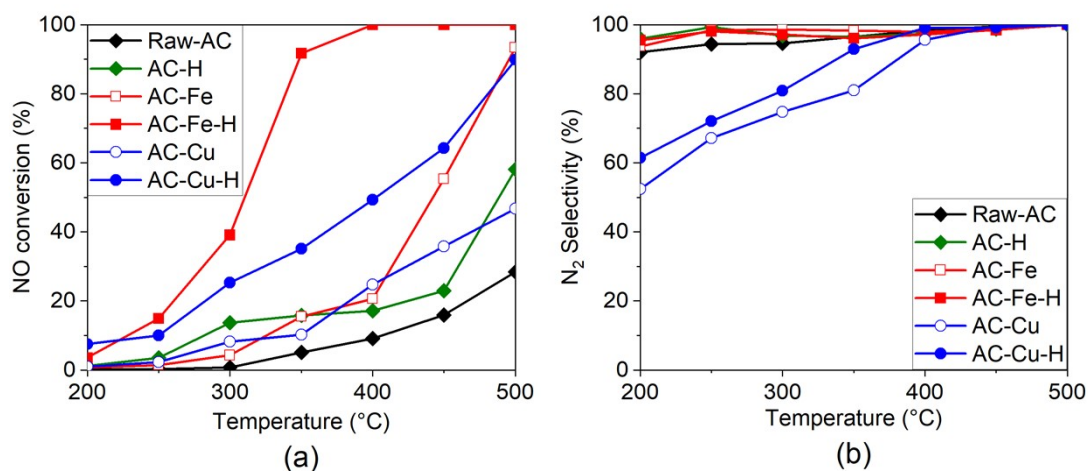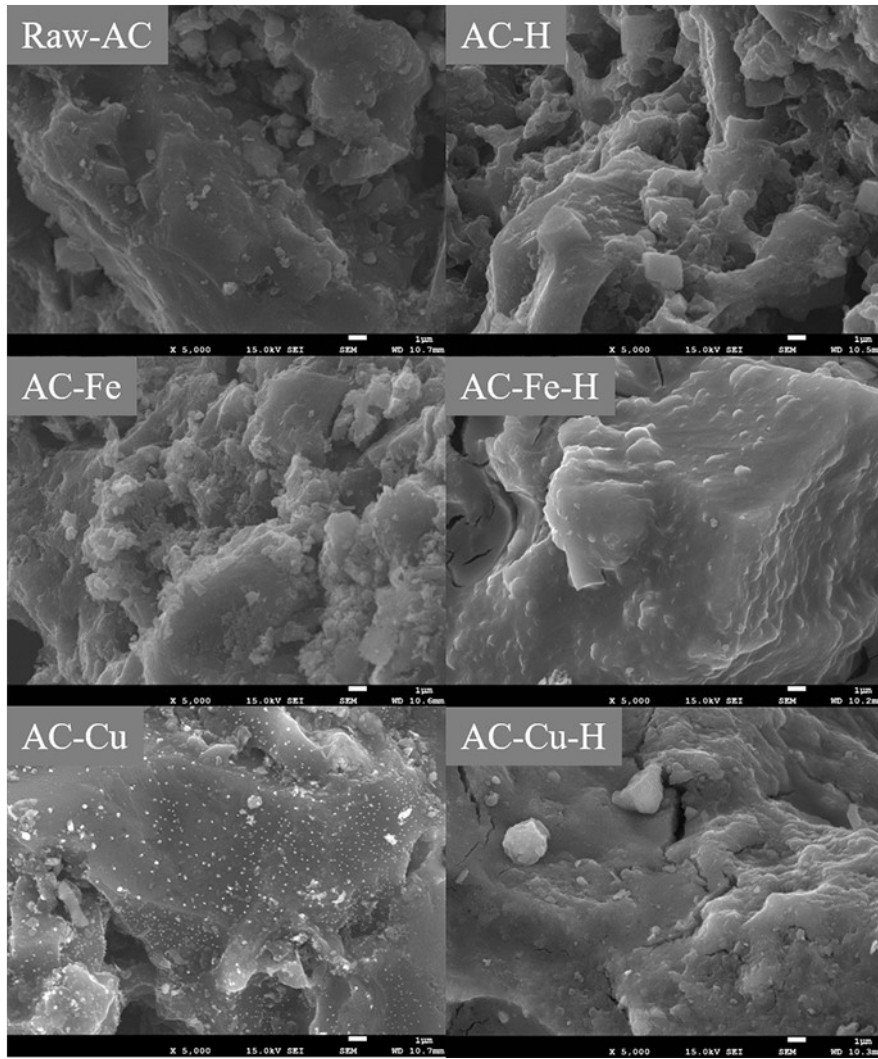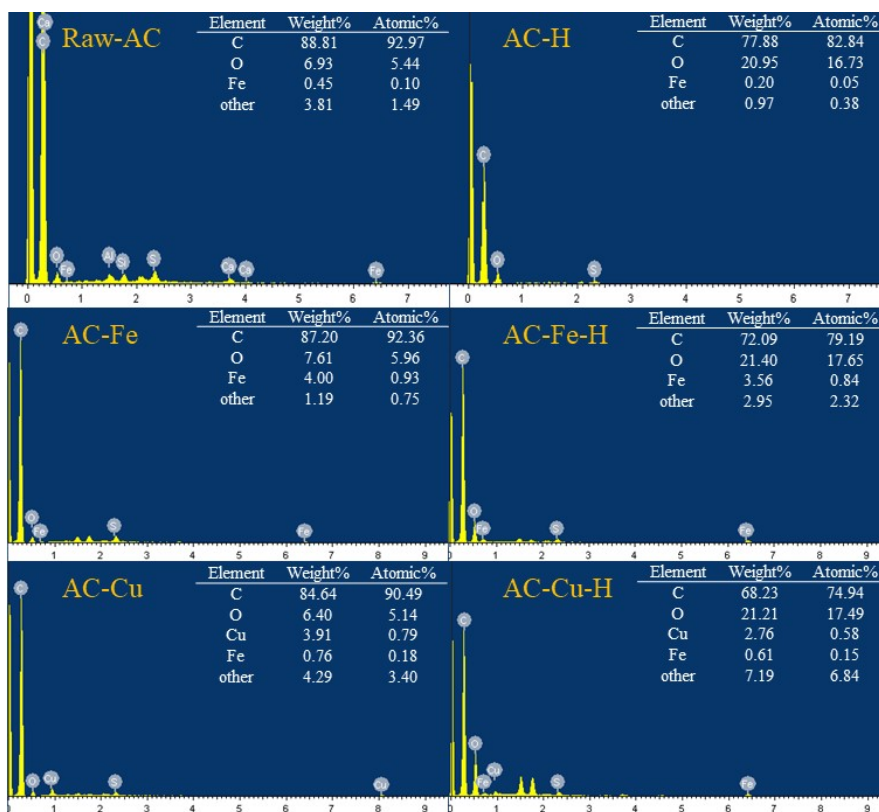

Figure S2 The (a) NO conversion and (b) N_2 selectivity on various AC samples with H_2O (Conditions: 500 ppm NO, 2% CO, 5% CO_2, 5% H_2O and N_2, 6000 h^{-1}, 200–500 °C).

The SEM results are shown in Fig. S3. Compared with Raw-AC, the surface roughness of AC-Fe and AC-Cu increases due to the deposition of metal salts on the surface. In addition, acid modification reduces the deposition salts on the surface of AC-Me, verifying that acid washing decreases the free metal species on the surface. The element content in Fig. S3(b) on the AC surface is detected by EDX. Acid modification significantly increases the O content from 6.93 wt% to 20.9 wt%, which proves that the acid modification successfully introduces oxygen-containing functional groups. The element mapping result in Fig. S3(c) shows that metal is uniformly dispersed on both AC-Me and AC-Me-H. The reason can be explained by the anchoring effect of oxygen-containing functional groups improving the dispersion of metal sites [1, 2].
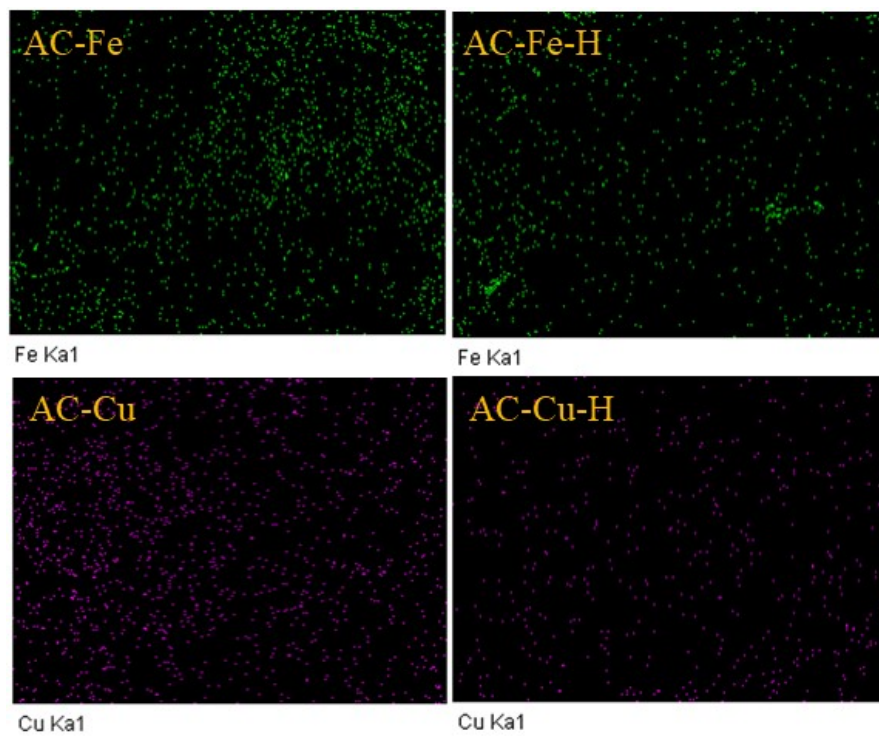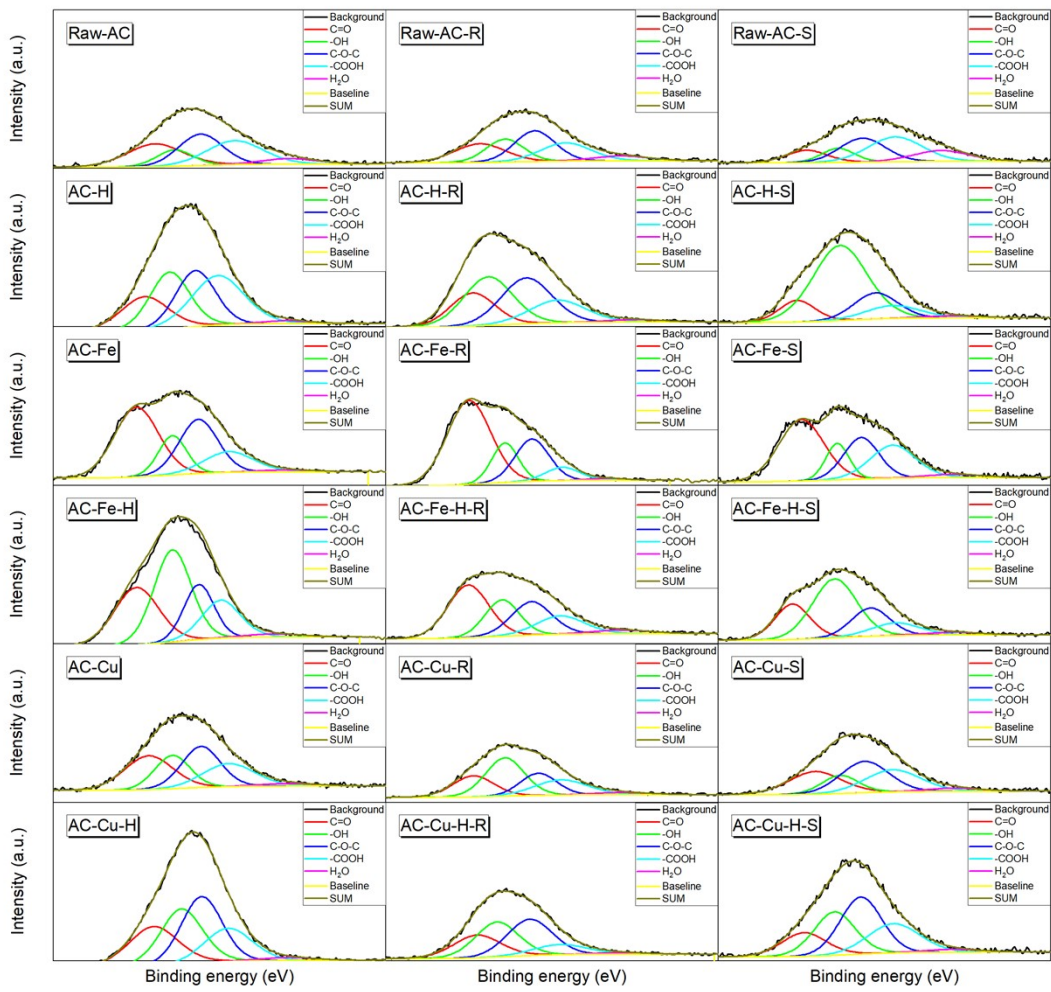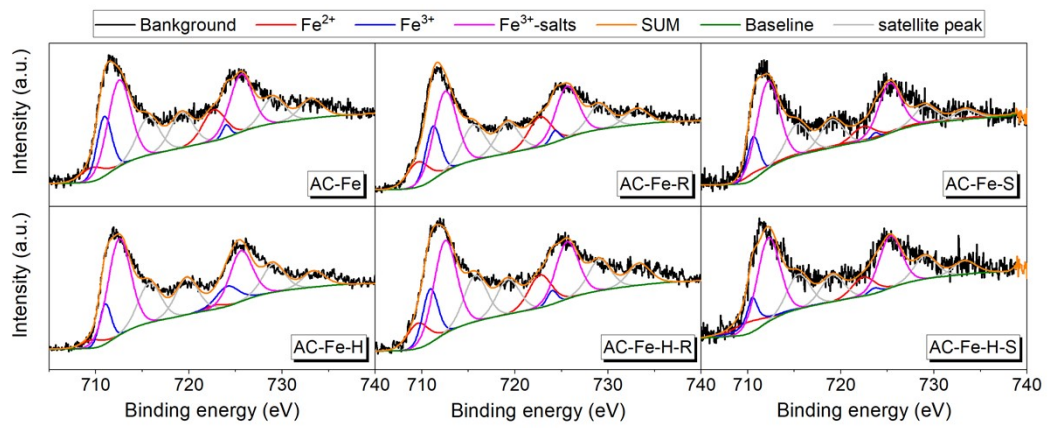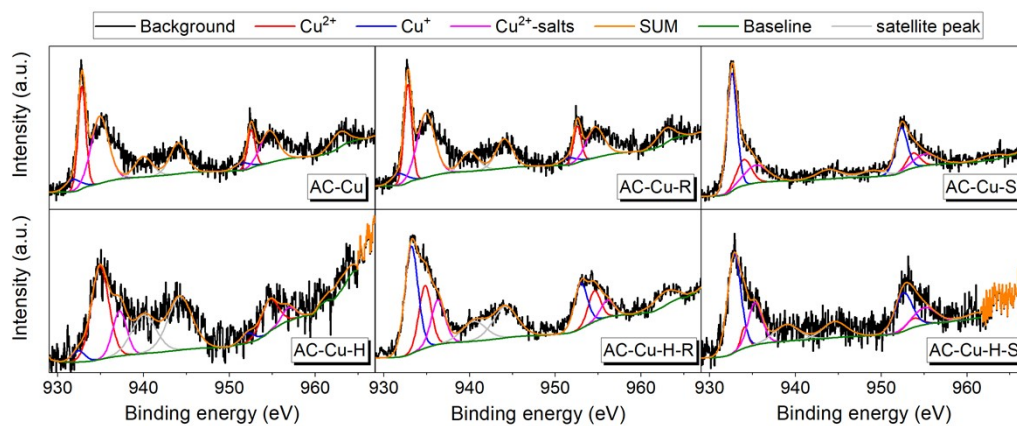
(a)

Raw-AC

Element	Weight%	Atomic%
C	88.81	92.97
O	6.93	5.44
Fe	0.45	0.10
other	3.81	1.49

AC-H

Element	Weight%	Atomic%
C	77.88	82.84
O	20.95	16.73
Fe	0.20	0.05
other	0.97	0.38

AC-Fe

Element	Weight%	Atomic%
C	87.20	92.36
O	7.61	5.96
Fe	4.00	0.93
other	1.19	0.75

AC-Fe-H

Element	Weight%	Atomic%
C	72.09	79.19
O	21.40	17.65
Fe	3.56	0.84
other	2.95	2.32

AC-Cu

Element	Weight%	Atomic%
C	84.64	90.49
O	6.40	5.14
Cu	3.91	0.79
Fe	0.76	0.18
other	4.29	3.40

AC-Cu-H

Element	Weight%	Atomic%
C	68.23	74.94
O	21.21	17.49
Cu	2.76	0.58
Fe	0.61	0.15
other	7.19	6.84

(b)

(c)

Figure S3 (a) SEM, (b) EDX and (c) mapping results on various AC samples.

(a)

(b)

Figure S4 (a) O 1s spectra, (b) Fe 2p spectra, and (c) Cu 2p spectra of various samples.
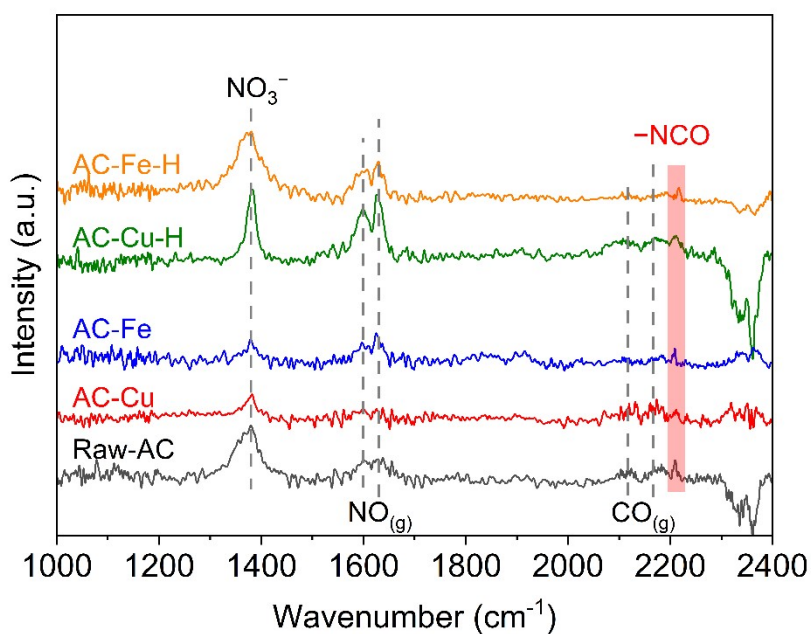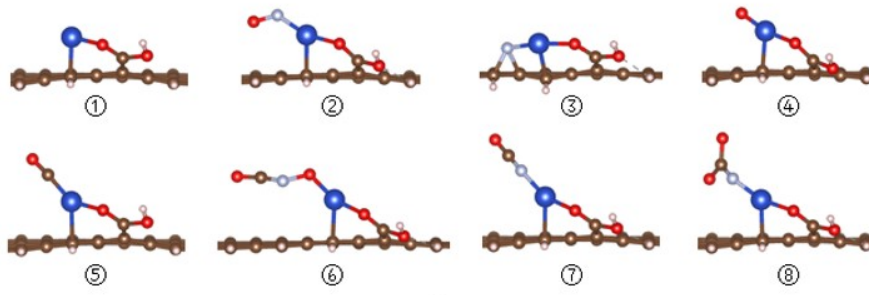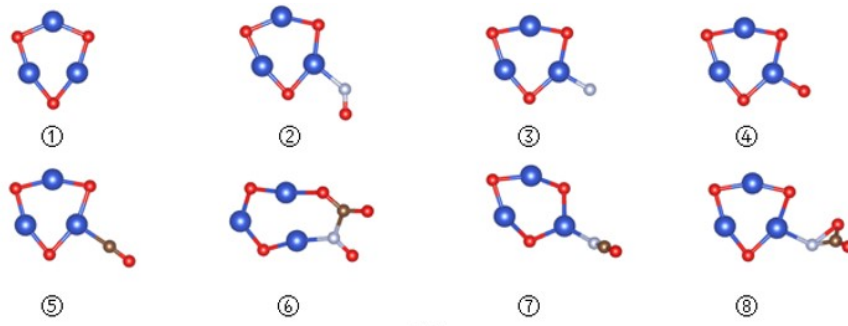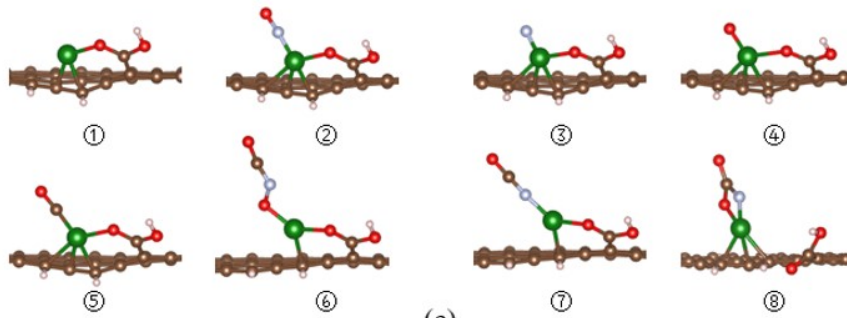

Figure S5 The in situ DRIFTS spectra of various samples (Conditions: 500 ppm NO and 250 ppm

CO and N_2, 250 °C)

(a)

(b)

(c)
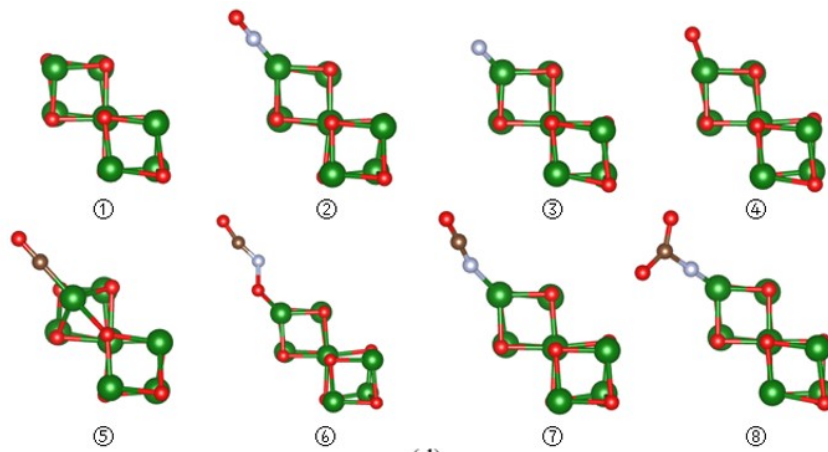
(d)

Figure S6 The adsorption of intermediates on various metal sites: (a) −COOH−Cu, (b) CuO, (c)

−COOH−Fe, and (d) Fe_3O_4. (Each metal site has 8 different surfaces with different intermediates: ①

clean, ② $^*NO$, ③ $^*N$, ④ $^*O$, ⑤ $^*CO$, ⑥ $^*ONCO$, ⑦ $^*NCO$, and ⑧ $^*NCO_2$.)
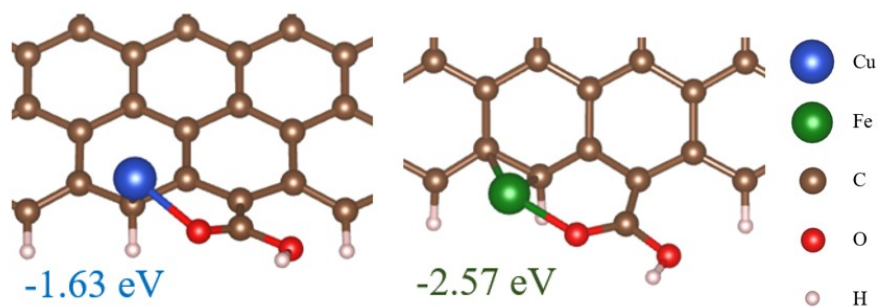

-1.63 eV   -2.57 eV

Cu	
Fe	
C	
O	
H	

Figure S7 The adsorption energy of Cu and Fe on binding metal sites.
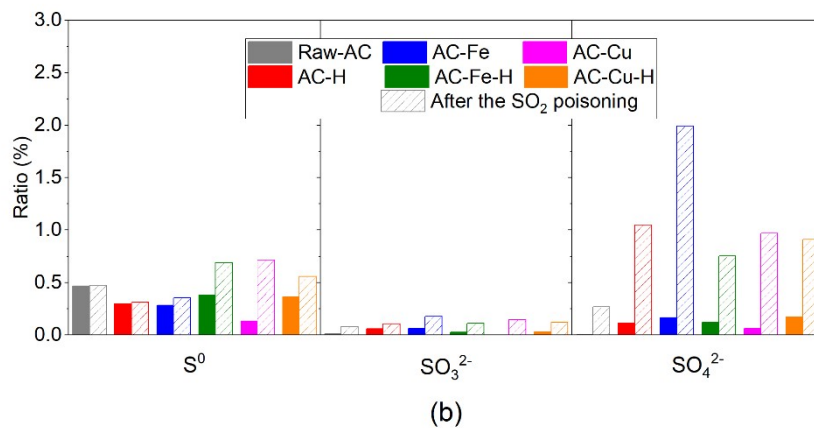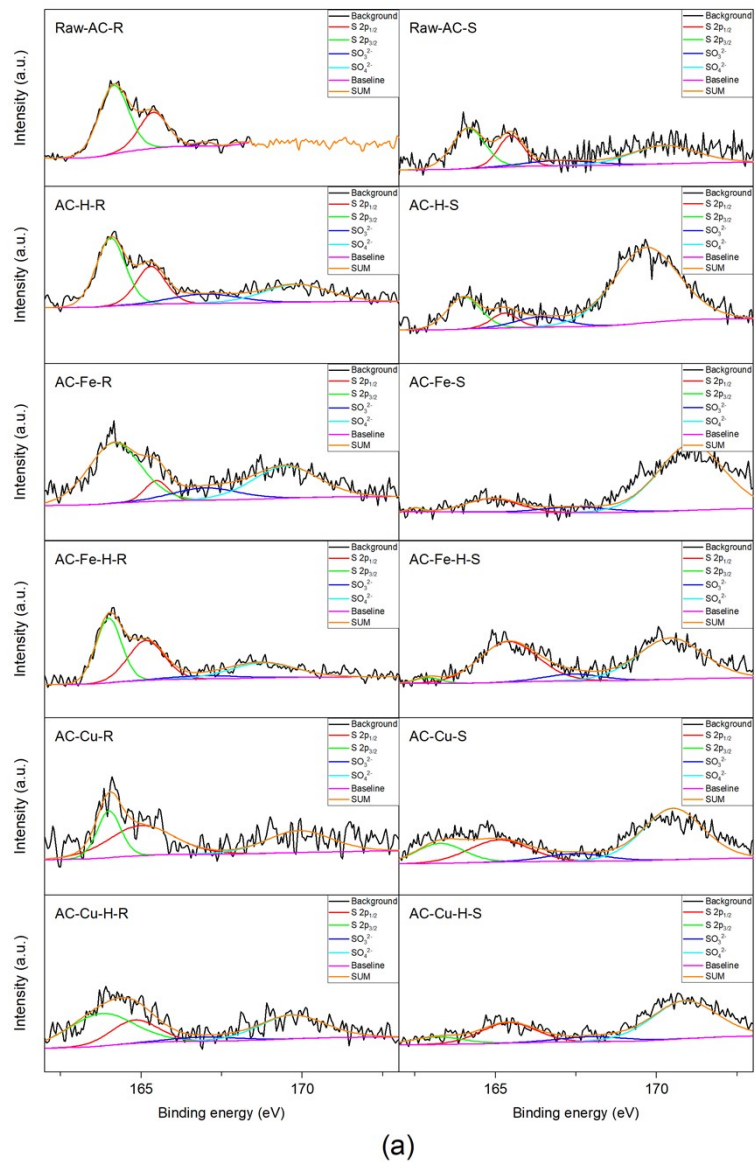
Figure S8 (a) S 2p spectra and (b) the proportion of various sulfur species from XPS on various

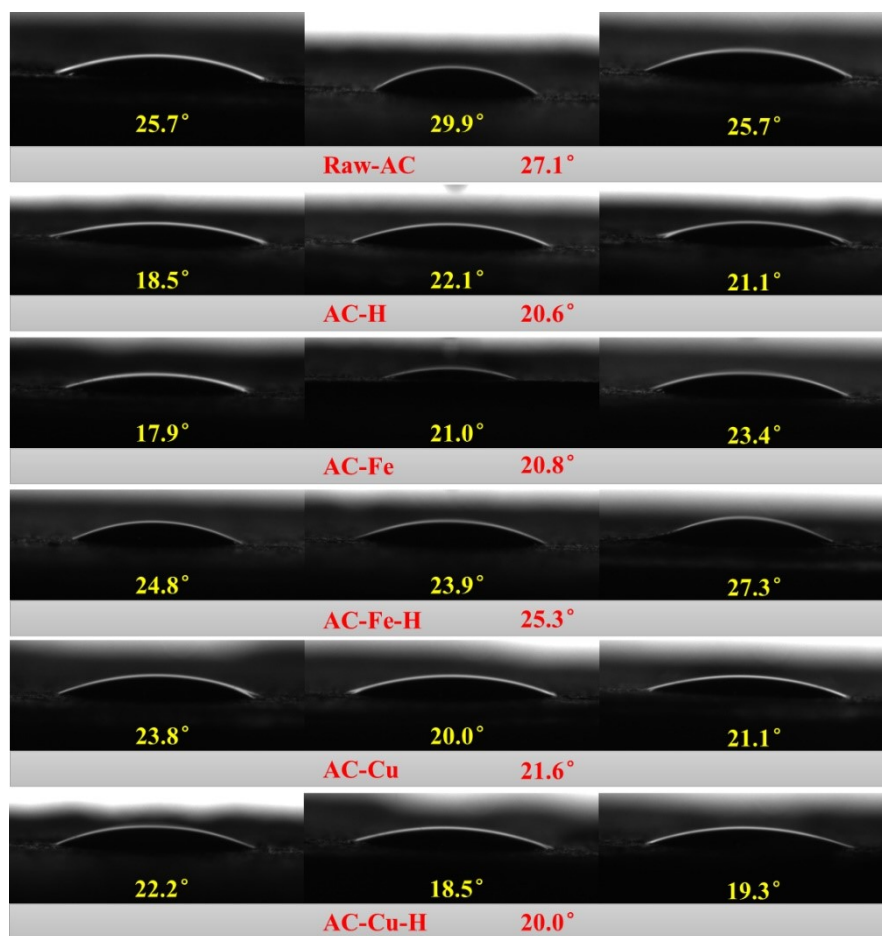samples before and after SO$_2$ poisoning.

Figure S9 The water contact angle on various samples.

References

1. Z. C. Xu, Y. R. Li, Y. T. Lin, Y. Wang, Q. Wang and T. Y. Zhu, *Chem. Eng. J.*, 2021, **419**.

2. Y.-M. Dai, T.-C. Pan, W.-J. Liu and J.-M. Jehng, *Appl. Catal. B-Environ.*, 2011, **103**.